Polymer Composites, **15**, 197–205 (1994)

INTERFACIAL TOUGHNESS AND ITS EFFECT ON COMPRESSION STRENGTH IN POLYCARBONATE/CARBON FIBER COMPOSITES

Paul R. Stone and John A. Nairn
Materials Science and Engineering Department
University of Utah, Salt Lake City, Utah 84112

ABSTRACT

Processing polycarbonate/carbon fiber composites for long times at high temperatures significantly improved adhesion between the matrix and the fibers. The interfacial properties were studied by measuring transverse fracture toughness, observing fracture specimens by scanning electron microscopy, and by monitoring composite cross-sections using atomic force microscopy. The processing treatment provided an ideal method for varying the properties of the interface without changing any other properties. We used this method to study the effect of interfacial properties on the axial compression properties of unidirectional composites. Both the compression strength and compression modulus increased significantly as the fiber/matrix adhesion improved. We concluded that improving interfacial adhesion increased compression properties by inhibiting fiber microbuckling.

Key Words: Interface, Toughness, Compression, Adhesion, Adsorption

INTRODUCTION

There are at least two important factors that can influence the fiber/matrix interface in thermoplastic matrix composites; neither factor has a significant effect on the interface in thermoset matrix composites. The first is matrix crystallinity. Fibers can act as nucleating agents and promote transcrystallinity in an interphase region between the fiber and the bulk matrix [1-9]. Transcrystallinity will almost certainly influence the mechanical properties of the interface (albeit not necessarily for the better [3]). Without transcrystallinity, or even with transcrystallinity, the second factor is adsorption of the polymer matrix onto the fiber. Adsorption is probably a prerequisite for achieving good fiber/matrix adhesion and even for achieving transcrystallinity [6]. Because the molecular weight of thermoplastic matrices is much higher than that of monomers in thermosetting matrices, the adsorption process can be much slower for thermoplastic matrices. It should not be surprising to find that long times at high temperature are required for promoting good adhesion in thermoplastic matrix composites [10,11].

Kardos *et al*. [1,2] found that annealing polycarbonate (PC) composites with random chopped carbon fibers at 245°C for three hours increases both the tensile strength and the modulus. Using electron diffraction, they attributed the increases to a transcrystalline region along the fibers.

Brady *et al*. [10,11] did annealing experiments on unidirectional PC/carbon fiber composites. They found that the interfacial toughness, as measured using a buckled plate specimen [11,12], increases with annealing time and increases faster at higher annealing temperatures. Because increased toughness could be induced by annealing above the melting point of PC (*i.e.,* above 220-260°C [13] for their conditions), they concluded that adsorption of the matrix onto the fiber, and not transcrystallinity, was the primary mechanism for the improved interface. They supported their adsorption interpretation by qualitatively fitting interface toughness data to Langmiur-type adsorption isotherms with kinetic parameters following Arrhenius activation energy theory [10].

Three important consequences follow from the work of Brady *et al*. [10,11]. First, adsorption of a thermoplastic matrix onto carbon fibers can be an important step in the processing of thermoplastic composites. If processing procedure provides insufficient time at high temperature, it is possible to get a composite in which the matrix has fully penetrated the fibers, but lack of adsorption has caused a poor fiber/matrix interface. In other words, results from optical microscopy alone are inadequate for assessing the processing procedure of thermoplastic composites. Second, adsorption of high-molecular-weight thermoplastics onto carbon fibers can be a slow process; it can take several hours at elevated temperatures. Third, annealing treatments provide a useful analytical tool for studying the effect of the interface on composite properties. Provided the annealing treatment does not change the bulk properties of the matrix (*e.g.,* by degradation or by changes in crystallinity), annealing of thermoplastic matrix composites provides a method for systematically changing the interface while all other composite properties remain the same.

In this study we used the annealing methods of Brady *et al*. [10,11] to further investigate the interface in unidirectional PC/carbon fiber composites. In analogy to previous results [10,11], our annealing treatments of PC/carbon fiber composites led to significant increases in transverse fracture toughness. Pressure, however, inhibited the toughness increase. Processing procedures that included long times at high temperature while maintaining a high pressure gave a smaller increase in toughness than similar processing procedures that used low pressure for most of the annealing time. To see the effect of interface on compression properties, we measured the longitudinal compression strength of a series of unidirectional composites with varying interfacial toughness. We found an increase in compression strength that paralleled the increase in interfacial toughness. We suggest that these results give experimental proof that the fiber/matrix interface has a direct and large effect on composite compression strength.

MATERIALS AND METHODS

12K Magnamite AS4 carbon fiber yarns (lot number 758-4B) were supplied by Hercules, Inc., Magna, Utah. AS4 is classified as a Type II intermediate strength fiber with a density of 1.796 g/cm^3. General Electric Lexan® polycarbonate was purchased as a roll of 3-mil film. Its measured density was 1.172 g/cm^3.

Unidirectional three-ply composite plates of PC/AS4 carbon fiber were fabricated by a film stacking technique. 6 inch X 6 inch steel plates with rounded edges were covered with 3-mil

DuPont Kapton® polyimide film and then with PC film. These plates were mounted in a hand-cranked, card-winding machine. AS4 yarns, whose width had been approximately doubled by air spreader bars, were wrapped around the plates using the card-winding mechanism. Two more layers of PC film and AS4 yarns were added followed by final layers of PC and Kapton® film. The Kapton® film provided a release layer that helped in sample removal from the steel plate. The steel plates with the three-ply composites were placed in a vacuum oven for a minimum of 12 hours at approximately 100°C to eliminate any moisture and to desorb volatiles before high-temperature processing. Each plate was then placed inside a vacuum bag of 3-mil Kapton® film, sealed with Tacky Tape (Schnee-Morehead Chemicals), and collapsed by application of laboratory vacuum. The vacuum-bagged composites were consolidated in a Carver Hot Press for selected processing times and temperatures under a pressure of 0.96 MPa (139 psi). The applied pressure was allowed to stabilize for approximately 2 minutes before starting the processing time clock. After selected processing times, the composites were cooled in the press, under pressure, to room temperature by passing laboratory distilled water through the channels inside the two heated platens. The composite cooling rate was approximately 25°C per minute. The thicknesses of the three-ply composites produced by this procedure ranged from 0.44 to 0.69 mm (17 to 27 mils). Fiber volume fractions were determined by measuring composite density and extrapolating between the density of carbon fiber (1.796 g/cm^3) and PC (1.172 g/cm^3). Composite densities were measured with a density gradient column prepared according to the guidelines of ASTM D-1505-68, Method C [14]. A water-calcium nitrate system was used to cover the desired density range of 1.3 - 1.5 g/cm^3.

We used transverse buckled plate tests [11,12] to evaluate the effect of processing time on the fiber/matrix interface. When a unidirectional composite is notched parallel to the fibers and transversely loaded in compression, it buckles at a critical load of

$$P_c = \frac{\pi^2 E w h^3}{12\ell^2} \tag{1}$$

where ℓ is length, $w = W\text{-}a$ is the total width (W) minus the notch depth (a), h is thickness, and E is the composite transverse modulus. During post-buckling, the displacement will increase until the crack propagates causing catastrophic failure. Chang and Donovan [12] showed that the energy release rate for crack growth is independent of the initial notch depth and given by the expression

$$G = 0.82\frac{Eh^2(\ell - x)}{\ell^2} f^*(\varepsilon) \tag{2}$$

where x is the chord length of the buckled plate (thus $\ell\text{-}x$ is total measured displacement), and

$$f^*(\varepsilon) = 0.158\varepsilon^2 + 0.229\varepsilon + 1 \tag{3}$$

is a function of strain $\varepsilon = (\ell\text{-}x)/\ell$. For low strains ($\varepsilon \leq 30\%$), ($\varepsilon$) is close to unity; we treated it as equal to unity in this study.

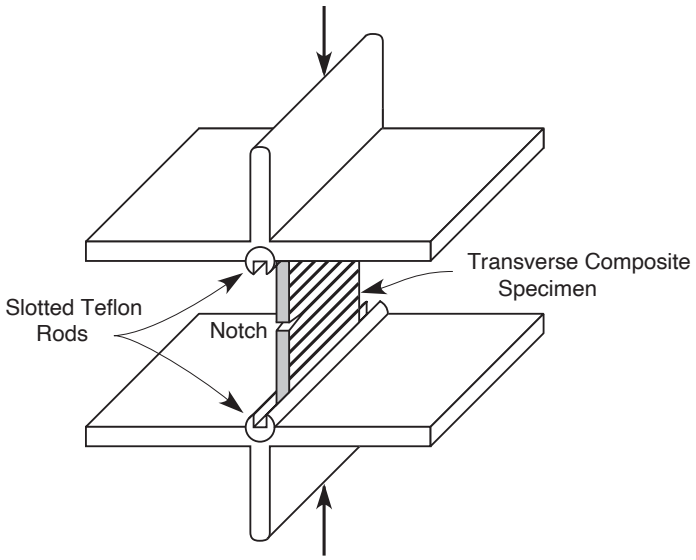

Fig. 1. Testing fixture for the buckled plate (BP) test. The transverse composite specimen (fibers perpendicular to the applied load) is compressed between two plates. The ends of the specimen are held in slotted Teflon® rods to allow free rotation of the ends.

Figure 1 shows the buckled plate (BP) testing apparatus. The BP specimen dimensions were 30 mm high by 15 mm wide. These dimensions were achieved by sanding with 220- and 400-grit silicon carbide sandpaper with the sample clamped in a stainless-steel jig. The upper and lower edges (parallel to the fiber direction) were further sanded gently to roundness with 400-grit silicon carbide sandpaper. A 1- or 2-mm deep notch parallel to the fiber direction was cut with a fresh razor blade along the mid-line of each specimen. These notched samples were mounted in slotted Teflon® rods and buckled in compression until fracture. Teflon® fluorinated ethylene-propylene rods, lubricated with Sprayon 708 TFE Dry Lube, were used to allow free rotation of the specimen ends. At the instant of fracture, Eq. (2) gives the transverse fracture toughness, G_c. Because G is independent of notch depth, those notches did not need to be measured. In principle, the modulus, E, can be calculated from the buckling load on the notched specimen before it fractures. This practice, however, tends to overestimate the *effective* buckling modulus [11]. As recommended in Ref. [11], we measured E from the buckling loads of unnotched plates.

Compression testing of the thin three-ply specimens was done using the method described in Refs. [15] and [16]. In brief, three-ply composites were cut into mini-dog-bone specimens 25 mm long by 20 mm wide. These specimens were embedded in a clear epoxy resin consisting of Dow Chemical DER 332 + Texaco Jeffamine D-230 + Texaco Accelerator 399 in the weight ratio of 10 : 3.5 : 1. These embedded specimens were loaded in compression with shim stock that matched the total embedded specimen thickness. To prevent premature buckling failures, the specimens were side supported during testing. Figure 2 shows the compression testing apparatus and specimen geometry.

The composite compression strength was calculated from the load at compression failure, P_{total}, by a simple rule-of-mixtures formula

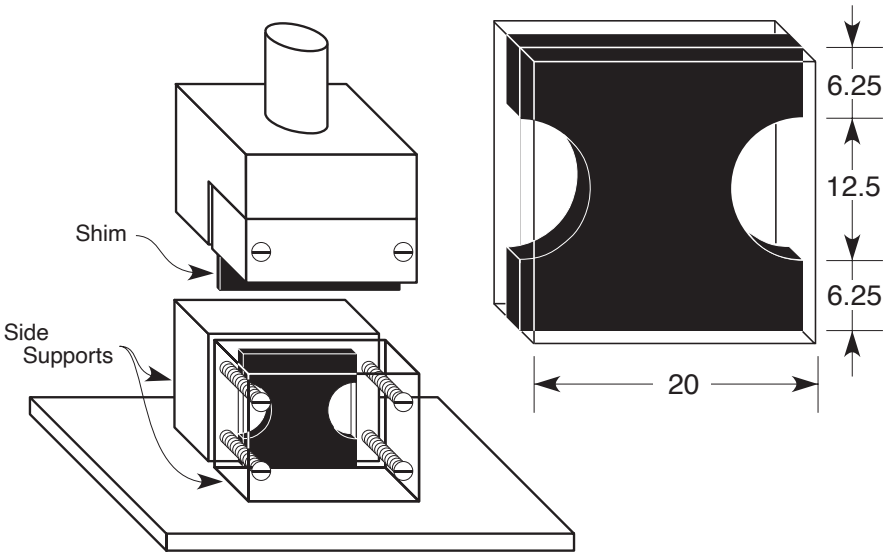

Fig. 2. The composite compression test fixture and a schematic of the embedded three-ply composite test specimen. The embedded three-ply composite specimens were positioned between two side supports. The rear side support was steel. A transparent, poly-methyl methacrylate front side support was used to permit observation of the failure process. Compression load was applied by a steel shim having a thickness matching that of the embedded three-ply composite specimen. The specimen dimensions are nominal dimensions in mm.

$$\sigma_c = \frac{P_{total} E_c}{E_c A_c + E_e A_e} \tag{4}$$

where E_c and E_e are the moduli of the three-ply composite and of the embedding epoxy. A_c and A_e are the cross-sectional areas of the three-ply composite and of the embedding epoxy at the location of compression failure. With the mini-dog-bone specimens, the compression failure was always at the point of minimum composite cross-sectional area. E_e was measured by compression tests on straight-sided specimens of pure epoxy [15,16]. E_c can be measured by compression tests on embedded straight-sided composite specimens followed by a simple rule-of-mixtures analysis [15,16]. For the home-made specimens in this study, we preferred to measure E_c on the same mini-dog-bone specimens used to measure compression strengths. The Appendix gives a simple analysis for estimating upper and lower bounds on the composite modulus. The upper and lower bounds were used with Eq. (4) to find upper and lower bounds on σ_c. Because E_c was always much greater than E_e, the bounds on σ_c calculated with Eq. (4) were always very tight. The error bars in Figs. 7 and 8 incorporate the bounds on σ_c and on E_c (See *Results and Discussion* section).

A servohydraulic Minnesota Testing Systems (MTS) Model 810 load frame under displacement control with a 2.5-kN reversible load cell was used for all testing. Data was collected on an IBM PC Model 5153 system using custom-developed software interfaced to an MTS Data Display Device. All buckled plate specimens were compressed at a rate of 0.33 mm/sec. All embedded, mini-dog-bone, compression specimens were loaded at a rate of 0.01 mm/sec. All experiments were done under ambient laboratory conditions.

Scanning electron micrographs (SEM) of BP specimens were collected on a Stereoscan 240 manufactured by Cambridge Instruments, Limited, of Cambridge, England. Samples were coated with gold using a Hummer V pulsed planar magnetron type sputtering system, manufactured by Technics Corporation of Alexandria, Virginia. The SEM specimens were prepared by mounting the BP specimen with the cracked region opened upward by bending the specimen into an inverted "V." Atomic force microscopy (AFM) force-modulation images of PC/carbon fiber composites were collected with a NanoScope II AFM manufactured by Digital Instruments, Inc., of Santa Barbara, California. Sample data were processed with force-modulation software.

RESULTS AND DISCUSSION

Transverse Fracture Toughness

Transverse fracture toughness measured in the buckled plate (BP) test characterizes some combination of crack growth through the matrix and crack growth along the fiber/matrix interface. The relative importance of matrix cohesive fracture and interfacial adhesive failure will depend on the relative magnitudes of the toughnesses for these two fracture mechanisms. In a series of specimens with identical matrices and nominally identical microstructures, it is logical to ascribe changes in transverse fracture toughness to changes in the interfacial properties of the composite. We thus used transverse buckling of notched, unidirectional composite specimens [11,12] to study the effect of processing conditions on interfacial properties.

We molded three-ply PC/carbon fiber composites at 300°C in a hot press under a constant consolidation pressure of 0.96 MPa. Figure 3 plots the transverse fracture toughness as a function of molding time. The toughness increased 133% from 1.71 kJ/m^2 for the 20-min composite to 3.98

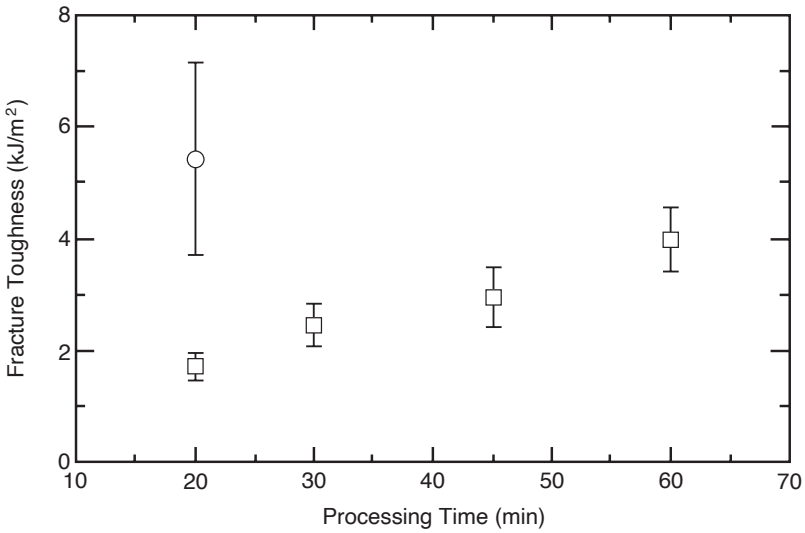

Fig. 3. Transverse fracture toughness vs. processing time of PC/carbon fiber composites processed at 300°C under a constant 0.96 MPa consolidation pressure. The circle is for a composite annealed for three hours at 275°C and 0.96 MPa after initial processing at 300°C and 0.96 MPa for 20 minutes. Error bars represent one standard deviation.

kJ/m^2 for the 60-min composite. Figure 3 shows an additional point (a circle) corresponding to 20-min composites that were further annealed for three hours at 275°C with the pressure maintained at 0.96 MPa. For this composite the fracture toughness was 217% larger (5.42 kJ/m^2) than the corresponding unannealed 20-min composite. These results indicated that longer molding times, at 300°C or at 275°C, give improvements in the interphase of PC/carbon fiber composites. The findings are similar to the results reported by Brady *et al*. [10,11], except that consolidation pressure was held high throughout the processing, and that the magnitude of the increase was smaller (133% *vs*. about 200% [10,11]).

We define two steps in the processes of making thermoplastic matrix composites — impregnation and adsorption. Impregnation is defined as the process of the matrix intermingling or interpenetrating with the fibers. Impregnation is a macroscopic step; optical micrographs of well-impregnated composites will show a uniform distribution of fibers within the matrix. Adsorption is the microscopic process of the matrix adsorbing onto the surface of the fiber; optical microscopy is not useful is studying adsorption. We agree with Brady *et al*. [10,11] that the improvements in transverse fracture toughness were due to the time required for PC matrix adsorption onto the carbon fibers not to changes in impregnation. Two observations support this conclusion. First, neither optical microscopy nor atomic force microscopy showed any obvious differences in the fiber/matrix distribution between the 20-min composites and the 60-min composites. Second, annealing without any applied pressure improved the interface. Pressure is probably a prerequisite for significant changes in impregnation of thermoplastic matrices. The improvements in interfacial toughness were also unrelated to crystallization of PC near the interface. Both the molding (300°C) and the annealing (275°C) temperatures were above the melting point of PC for these annealing conditions [13]. For all processing conditions, the final step was to cool rapidly to room temperature at about 25°C/min. Thus, even if the difficult-to-crystallize PC could form crystals, the level of crystallinity would be relatively constant from specimen to specimen. After eliminating impregnation and crystallinity, the remaining mechanism for improvements in interfacial toughness is matrix adsorption onto the fiber.

We supplemented the work of Brady *et al*. [10,11] by studying the effect of composite consolidation pressure. Some three-ply, PC/carbon fiber composites were molded at 300°C for 60 minutes. During molding, the composites were under a pressure of 0.96 MPa for a variable amount of time and under vacuum-bag pressure only for the remaining time. Figure 4 plots the transverse fracture toughness as a function of time under 0.96 MPa pressure. There was some benefit to applying consolidation pressure. The toughness after 2 minutes of pressure was higher than the toughness achieved without any applied pressure. After the initial improvement in toughness, however, no further benefit was found by continuing the applied consolidation pressure. Rather, continued application of pressure caused the composite toughness to decrease. A possible explanation for these results is a pressure effect on adsorption of the matrix onto the fiber surface. Pressure could inhibit adsorption either by increasing the melt viscosity of PC or by causing fiber/fiber contact zones that cannot be penetrated by the matrix.

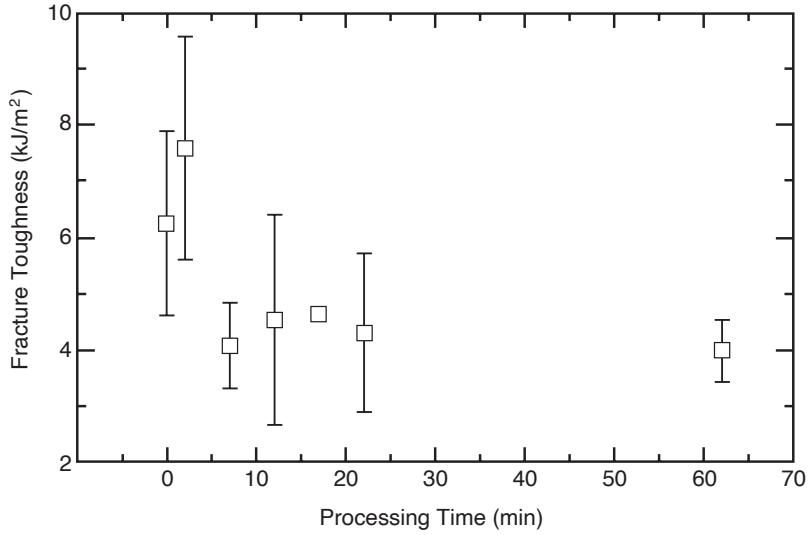

Fig. 4. Transverse fracture toughness vs. composite processing pressure hold time at 0.96 MPa. Vacuum-bag pressure only is defined as zero hold time. All composites were processed at 300°C for 60 minutes. Error bars represent one standard deviation.

Microscopy

SEM micrographs in Fig. 5 are consistent with an interpretation of improved fiber/matrix adhesion following annealing treatments. Figure 5A shows a composite that was processed at 300°C for 20 minutes under a pressure of 0.96 MPa. The fibers appear bare, indicating weak adhesion. Figure 5B shows a composite that was processed at 300°C for 20 minutes under a pressure of 0.96 MPa and 40 minutes under vacuum bag pressure only. This 60-min composite showed more evidence of the PC matrix sticking to the fibers and elongating during failure.

Maivald *et al*. [17] used atomic force microscopy (AFM) in a force-modulation mode to image surface elasticity in an epoxy resin composite in cross-section. In brief, a nano-probe was moved over the surface of an object and the force was held approximately constant through a feedback loop. At each scanned position, a small motion with an amplitude of about 25 nm, Δz_m, was introduced into the z-direction of the specimen position. This motion caused a small motion of the nano-probe of Δz_d. The magnitude of $\Delta z_d/\Delta z_m$ provides a measure of surface elasticity. The quantity $\Delta z_d/\Delta z_m$ approaches one over hard areas and is smaller over soft areas. Thus, imaging $\Delta z_d/\Delta z_m$ over the scanned surface images changes in surface elasticity [17]. The resolution of AFM is more than adequate to image 7-μm carbon fibers.

We used force-modulation AFM to image cross-sections of composites processed under different conditions. The AFM images of polished cross sections of PC/carbon fiber composites are shown in Fig. 6. The force-modulation surface images were obtained by scanning in a raster pattern over a selected region of the composite. The area imaged was 15796 nm X 15796 nm. Our qualitative interpretation of the AFM images focused on image contrast as a descriptor of differences in fiber/matrix adsorption. Figure 6A shows a 20-min composite. There is sharp contrast between the fibers and the matrix. We attempted no quantitative analysis, but the AFM

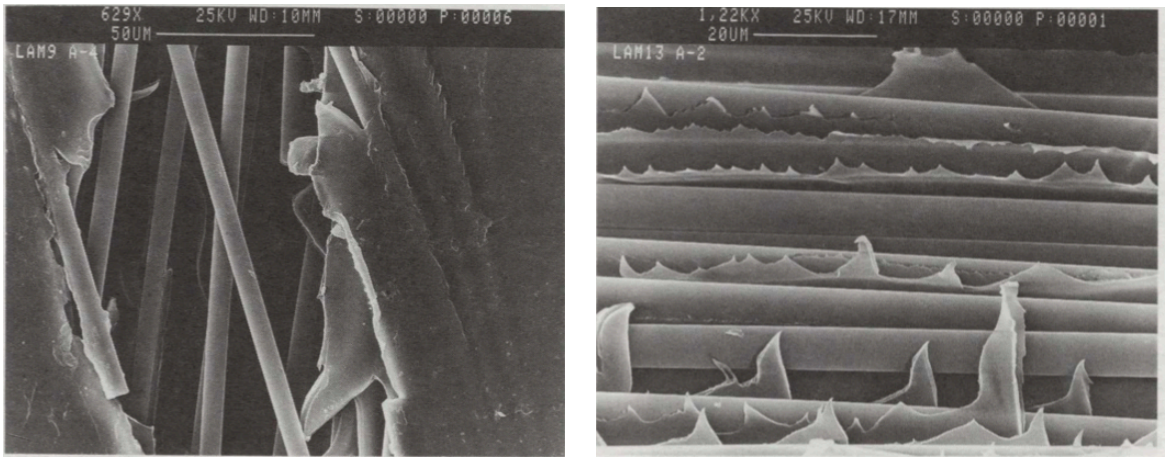

A B

Fig. 5. SEM micrographs of the fracture surfaces of buckled plate specimens. A: Specimen that was processed for 20 minutes at 300°C and 0.96 MPa. B: Specimen that was processed for 60 minutes at 300°C. The first 20 minutes were at 0.96 MPa. The remaining 40 minutes were at vacuum-bag pressure only.

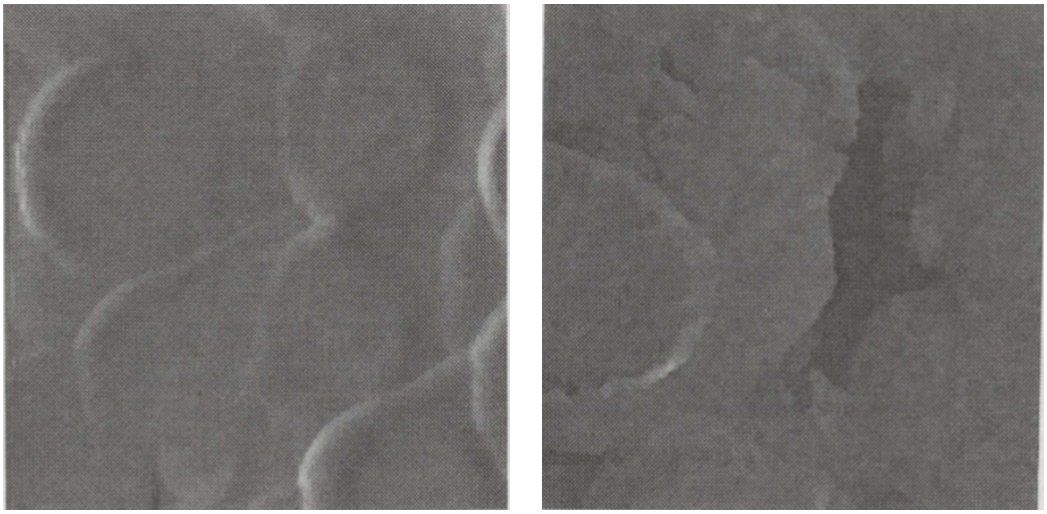

A B

Fig. 6. A. An AFM force-modulation image of a composite processed for 20 minutes at 300°C under a consolidation pressure of 0.96 MPa. B. An AFM force-modulation image of a composite processed for 60 minutes at 300°C under a consolidation pressure of 0.96 MPa. The images in both A and B correspond to square areas that were 15.796 μm X 15.796 μm.

probe was capable of detecting the interfacial region. In comparison, the 60-min composite in Fig. 6B shows much lower contrast. The process of the matrix adsorbing onto the fiber made the interfacial region more transparent to the AFM probe. The AFM contrast changes at the interface correlated with the changes in interfacial properties measured by the BP test. Similar optical or SEM micrographs at similar magnifications would show no differences between the 20-min composite and the 60-min composite. In other words, AFM imaging is a potential tool for making direct observations of changes at the interface.

Compression Strength Testing

The effect of processing time on the interfacial properties of PC/carbon fiber composites has important implications about the optimal processing of thermoplastic matrix composites. A side-benefit is that processing time provides a method for controlling the interface. By processing composites for different amounts of time it is possible to get a series of specimens in which the only variable is the interfacial toughness. The matrix, the fiber, and the nominal microstructure (or impregnation) will be identical while only the interface is changing. Such a series of composites provides ideal specimens for studying the effect of the interface on any composite property. In this section we discuss the effect of the interface on compression strength.

We molded three-ply composites, identical to those used for Fig. 3, at 300°C under a constant consolidation pressure of 0.96 MPa for variable amounts of time. The compression strength was measured, as described in the *Materials and Methods* section, by embedding mini-dog-bone specimens in a clear epoxy and end-loading side-supported specimens in compression. Figure 7 plots the compression strength as a function of composite processing time. The plot shows a significant increase in PC/carbon fiber compression strength with increased processing time. This increase in strength parallels the increase in interfacial toughness shown in Fig. 3 and suggests a direct relation between interfacial properties and compression strength.

The 0° compression strengths reported for several commercial unidirectional AS4 carbon fiber/thermoplastic composites fall in the range of 0.9-1.4 GPa [18]. In contrast, our results range from 0.32 GPa to 0.58 GPa. These differences mainly reflect the fiber volume fractions. Commercial composites normally strive for high volume fractions — $V_f = 60\%$ or higher. Our home-made composites had fiber volume fractions of 35±5%.

Polycarbonate is a matrix of relatively low modulus. In PC/carbon fiber composites under 0° longitudinal compression, it is therefore likely that fiber buckling dominates or influences the failure mode [19,20]. In our test, the bulk matrix properties were constant, and only the interphase

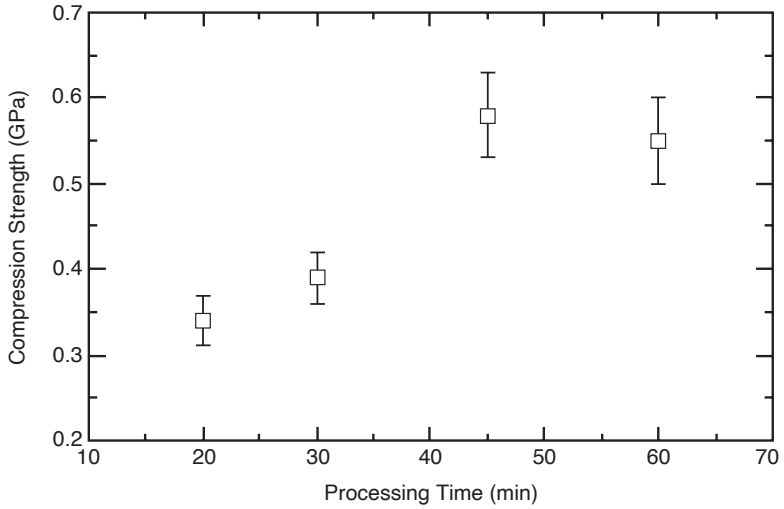

Fig. 7. Longitudinal compression strength vs. processing time of PC/carbon fiber composites processed at 300°C and 0.96 MPa consolidation pressure. Error bars represent one standard deviation.

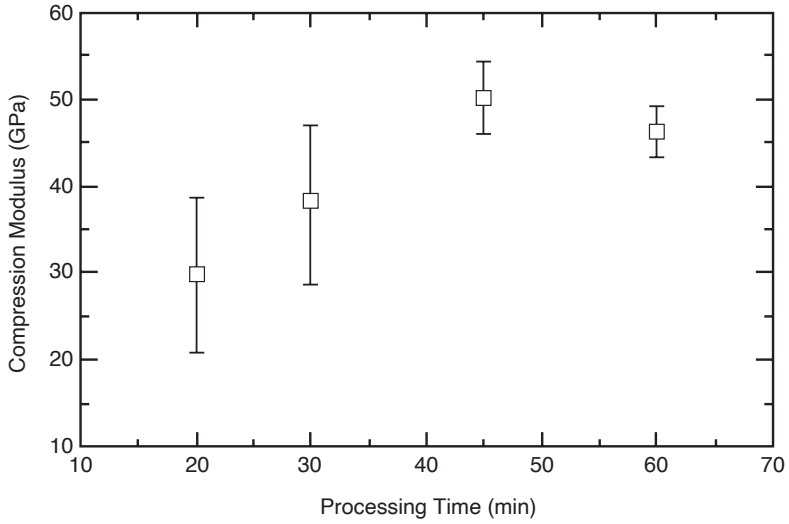

Fig. 8. Longitudinal compression modulus vs. processing time of PC/carbon fiber composites processed at 300°C and 0.96 MPa consolidation pressure. Error bars represent one standard deviation.

properties were changed by the processing time. The increase in compression strength for PC/carbon fiber composites with processing time thus indicates that fiber buckling failure was inhibited by improved interfacial properties and improved fiber-matrix bonding.

The longitudinal compression modulus data are plotted against composite processing time in Fig. 8. An unexpected result was a significant increase in compression modulus with processing time. We suggest that the low modulus for composites with a poor fiber/matrix interface (short processing times) was caused by fiber microbuckling. Thus, the same mechanism that was responsible for a low compression strength was also responsible for a low compression modulus. As the interface was improved by longer processing times, the microbuckling mechanism was inhibited and both the compression strength and the compression modulus increased. Other possible variables, such as bulk matrix modulus, were disregarded because only the fiber/matrix interface was altered by varying the processing conditions. Tension testing is one way to verify the effect of microbuckling on compression modulus. Under tensile loading, fiber buckling cannot occur. Therefore, unlike the compression modulus, the tensile modulus should be independent of composite processing time. This work is in progress.

CONCLUSIONS

In agreement with previous results by Brady *et al*. [11,12], annealing PC/carbon fiber composites for long times at high temperature increases the toughness of the fiber/matrix interface. Besides annealing temperature, pressure is also an important processing variable. Using high pressure for too long limits improvements in the interface. Avoiding pressure altogether, however, also limits the interfacial properties. We suggest that pressure must be used initially until the matrix fully impregnates with the fibers. The optimal processing conditions are 1) to remove the pressure immediately after impregnation, and 2) to allow enough time at high temperature to permit matrix adsorption onto the fibers.

Three pieces of experimental evidence suggest that the interface changes with high-temperature annealing. First, transverse fracture toughness measured by a BP test increases with annealing time. Second, SEM micrographs suggest more matrix adhering to the fibers in composites that were annealed for long times. Third, AFM force-modulation images indicate changes in the interfacial region that are associated with the elastic properties of the interface. The AFM images alone cannot differentiate between good and poor interface properties. AFM is interesting, however, as a potential tool for direct observation of interfacial regions.

This study is possibly the first one to measure compression strength where the *only* material variable is interfacial toughness. By using annealing treatments to change the interfacial toughness, we were able to isolate effects of the fiber/matrix interface — that is, we varied the interfacial toughness while holding other composite material properties constant. Both the compression strength and the compression modulus increased significantly as the fiber/matrix interface improved. We suggest that inhibition of fiber microbuckling by an improved interface played a role in increasing the compression strength and modulus properties.

The performance of PC/carbon fiber composites is perhaps representative of thermoplastic composites. Thus, long processing times, similar to those used for thermosetting systems, may be required for achieving satisfactory fracture toughness and compression strength in thermoplastic composites. Pressure is also an important processing variable. Too much pressure for too long lengthens the time required to manufacture good composites.

ACKNOWLEDGMENTS

Funding for this project was provided under NASA Contract NAS1-18883. Eric W. Stroup (University of Utah) is gratefully acknowledged for generating the AFM images.

APPENDIX

The compression test in Fig. 2 uses a mini-dog-bone composite specimen of modulus E_c embedded in a block of epoxy with modulus E_e. During compression tests we measured the embedded specimen moduli, denoted as E_{eff}. To account for possible specimen-to-specimen variations in E_c in our home-made composites, it was desirable to measure E_c for each compression test specimen. This appendix gives a simple procedure for estimating upper and lower bounds on E_c from knowledge of E_e, E_{eff}, and specimen dimensions.

For model 1 (Fig. A-1A) we consider a specimen of length ℓ, width W, thickness t, and cross-sectional area A, whose stiffness varies along its length. By making horizontal slices, we divide it into a chain of disks where each disk has the same cross-sectional area but a different modulus. Modeling the chain of disks as springs in series and passing to the limit of an infinite number of disks, the specimen modulus is

$$\frac{1}{E_{eff}} = \frac{1}{\ell}\int_{-\ell/2}^{\ell/2} \frac{1}{E(x)}dx \qquad \text{(A1)}$$

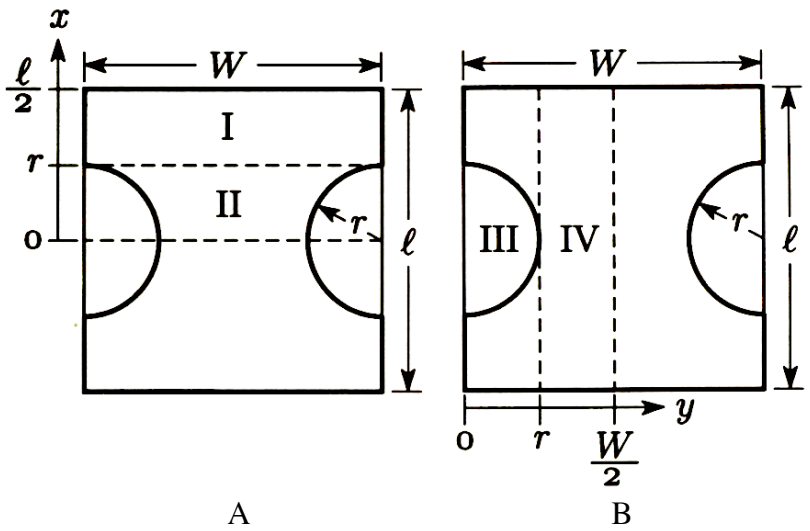

Fig. 6. Regions of the embedded mini-dog-bone composite specimen used to calculate upper and lower bound composite moduli. A. Regions for the chain-of-disks model (model 1). B. Regions for the rack-of-disks model (model 2).

where $E(x)$ is the modulus as a function of position along its length. Model 1 splits the symmetric compression specimen into two regions. In region I, the composite cross-sectional area is constant. Therefore, $E(x)$ is constant; by a rule-of-mixtures analysis it is

$$E(x) = E_R = \frac{E_e(t - t_c) + E_c t_c}{t} \qquad \text{for } r < x < \ell/2 \quad \text{(A2)}$$

where t_c is composite thickness. The cut-out in region II is an arc of radius r. By a rule-of-mixtures analysis, the modulus at position x is

$$E(x) = \frac{E_e(A - A_c(x)) + E_c A_c(x)}{A} = E_R\left(1 + \beta_1\sqrt{r^2 - x^2}\right) \qquad \text{for } 0 < x < r \quad \text{(A3)}$$

where $A_c(x)$ is the cross-sectional area of the composite at position x and

$$\beta_1 = -\frac{2t_c}{tW}\,\frac{E_c - E_e}{E_R} \qquad \text{(A4)}$$

Combining Eqs. (A1), (A2), and (A3), the specimen modulus by model 1 is

$$\frac{1}{E_{eff}} = \frac{1}{\ell E_R}\left(\ell - 2r + 2I(\beta_1)\right) \qquad \text{(A5)}$$

where

$$I(\beta) = \int_0^r \frac{dx}{1 + \beta\sqrt{r^2 - x^2}} \qquad \text{(A6)}$$

For model 2 (Fig. A-1B) we consider a specimen whose stiffness varies along its width. By making vertical slices, we divide it into a rack of disks where each disk has the same cross-sectional area but a different modulus. Modeling the rack of disks as springs in parallel and passing to the limit of an infinite number of disks, the specimen modulus is

$$E_{eff} = \frac{1}{W}\int_{-W/2}^{W/2} E(y)\ dy \tag{A7}$$

Model 2 splits the symmetric compression specimen into two regions. In region IV, the composite longitudinal-sectional area is constant and $E(y)$ is equal to E_R (a constant). We model each position in region III as three springs in series. The middle spring is the region of pure embedding epoxy $\left(|x| < \sqrt{r^2 - y^2}\right)$. Its length is

$$\ell_2 = \sqrt{r^2 - y^2} \tag{A8}$$

and its modulus is E_e. The top and bottom springs are regions of composite embedded in epoxy $\left(|x| > \sqrt{r^2 - y^2}\right)$. Their lengths are

$$\ell_1 = \ell_3 = \ell/2 - \sqrt{r^2 - y^2} \tag{A9}$$

and their moduli are both E_R. Analyzing the three springs in series, the modulus in region III is

$$E(y) = \frac{E_R}{1 + \beta_2\sqrt{r^2 - x^2}} \qquad \text{for } 0 < y < r \tag{A10}$$

where

$$\beta_2 = \frac{2}{\ell}\frac{E_R - E_e}{E_e} \tag{A11}$$

Combining Eqs. (A7) and (A10), the specimen modulus by model 2 is

$$E_{eff} = \frac{E_R}{W}\left(W - 2r + 2I(\beta_2)\right) \tag{A12}$$

The same $I(\beta)$ function appears in each model. It can be integrated in closed form:

$$I(\beta) = \frac{1}{2\beta}\left(\pi - \frac{4}{\sqrt{1 - \beta^2 r^2}}\ \tan^{-1}\ \frac{\sqrt{1 - \beta^2 r^2}}{1 - \beta r}\right) \qquad \text{for } 1 - \beta^2 r^2 > 0 \tag{A13}$$

$$I(\beta) = r \qquad \text{for } 1 - \beta^2 r^2 = 0 \tag{A14}$$

$$I(\beta) = \frac{1}{2\beta}\left(\pi - \frac{2}{\sqrt{\beta^2 r^2 - 1}}\ln\frac{1 + \beta r + \sqrt{\beta^2 r^2 - 1}}{1 + \beta r - \sqrt{\beta^2 r^2 - 1}}\right) \qquad \text{for } 1 - \beta^2 r^2 < 0 \tag{A15}$$

To find the composite modulus for a mini-dog-bone composite embedded in an epoxy, we numerically solve Eqs. (A5) and (A12) for E_c. We claim (without proof) that the series model (model 1) gives a lower bound to E_c and that the parallel model (model 2) gives an upper bound to E_c. These upper and lower bound moduli can then be substituted into Eq. (4) to find upper and lower bounds for the composite compression strengths.

REFERENCES

1. J. L. Kardos, "Regulating the Interface in Graphite/Thermoplastic Composites," *J. Adhesion*, **5**, 119 (1973).
2. J. L. Kardos, F. S. Cheng, and T. L. Tolbert, "Tailoring the Interface in Graphite-Reinforced Polycarbonate," *Polym. Eng. & Sci.*, **13**, 455 (1973).
3. T. Bessel and J. B. Shortall, "The Crystallization and Interfacial Bond Strength of Nylon 6 at Carbon and Glass Fibre Surfaces," *J. Mat. Sci.*, **10**, 2035 (1975).
4. P. O. Frayer and J. B. Lando, "Polymerization in Electric Fields of Hexamethylene-diammonium Adipate Crystallized on Graphite Fibers," *J. Polym. Sci., Polym. Lett. Ed.*, **10**, 29 (1972).
5. F. Tuistra and E. Baer, "Epitaxial Crystallization of Polyethylene on Graphite," *J. Polym. Sci., Polym. Lett. Ed.*, **8**, 861 (1970).
6. S. Y. Hobbs, "Row Nucleation of Isotactic Polypropylene on Graphite Fibers," *Nature Phys. Sci.*, **234**, 12 (1971).
7. D. Campbell and M. M. Qayyum, "Melt Crystallization of Polypropylene: Effect of Contact with Fiber Substrates," *J. Polym. Sci., Polym. Phys. Ed.*, **18**, 83 (1980).
8. D. Campbell and M. M. Qayyum, "Enhanced Fracture Strain of Polypropylene by Incorporation of Thermoplastic Fibres," *J. Mat. Sci.*, **12**, 2427 (1977).
9. Y. C. Lee and R. S. Porter, "Crystallization of Poly(etheretherketone) PEEK in Carbon Fiber Composites," *Polym. Eng. & Sci.*, **26**, 633 (1986).
10. R. L. Brady and R. S. Porter, "Interfacial Crystallization and Adsorption in Polycarbonate/Carbon Fiber Composites," *J. Thermoplastic Comp.*, **2**, 164 (1989).
11. R. L. Brady, R. S. Porter, and J. A. Donovan, "A Buckled Plate Test to Measure Interfacial Toughness in Composites," *J. Mat. Sci.*, **24**, 4138 (1989).
12. P. Chang and J. A. Donovan, "Crack Size Independence of the Crack Driving Force in the Buckled Plate Specimen," *J. Mat. Sci.*, **24**, 816 (1989).
13. J. M. Jonza and R. S. Porter, "High-Melting Bisphenol-A Polycarbonate from Annealing of Vapor Induced Crystals," *J. Polym. Sci., Polym. Phys. Ed.*, **24**, 2459 (1986).
14. "Standard Test Method for Density of Plastics by the Density-Gradient Technique," ASTM Designation D1505-68, Method C (Continuous Filling with Liquid Entering Gradient Tube Becoming Progressively More Dense), American Society for Testing and Materials (1968).
15. J. B. Ha and J. A. Nairn, "Compression Failure Mechanisms of Single-Ply Unidirectional Carbon-Fiber Composites," *SAMPE Quarterly*, **23**, 29 (1992).

16. J. B. Ha, "The Compression Study of Unidirectional Single-Ply Composites," PhD Thesis, University of Utah, June 1992.
17. P. Maivald, H. J. Butt, S. A. C. Gould, C. B. Prater, B. Drake, J. A. Gurley, V. B. Elings, and P. K. Hansma, "Using Force Modulation to Image Surface Elasticities with the Atomic Force Microscope," *Nanotechnology*, **2**, 103 (1991).
18. D. C. Leach, " Continuous Fibre Reinforced Thermoplastic Matrix Composites," in *Advanced Composites*; 43 (Ed. I. K. Partridge, Elsevier Applied Science: London, 1989).
19. B. W. Rosen, "Mechanics of Composite Strengthening," in *Fiber Composite Materials*, 37 (American Society of Metals, Metals Park, Ohio, 1964).
20. P. D. Ewins and R. T. Potter, "Some Observations on the Nature of Fibre Reinforced Plastics and Implications for Structural Design," *Phil Trans. R. Soc. Lond.*, **A294**, 507 (1980).